

Push-pull resonant DC-DC isolated converter

S. JALBRZYKOWSKI* and T. CITKO

Faculty of Electrical Engineering, Białystok University of Technology, 45D Wiejska St. 15-351 Białystok, Poland

Abstract. A new concept of a DC-DC converter with galvanic isolation is proposed in this paper. The converter belongs to the class E resonant converters controlled by pulse width modulation via frequency regulation (PWM FM). Due to the possibility of operation in the boost and buck modes, the converter is characterized by a high range of voltage gain regulation. The principle of converter operation described by mathematical equations is presented. The theoretical investigations are confirmed by p-spice model simulations and the measurement of an experimental model of 1kW laboratory prototype.

Key words: push-pull, DC-DC resonant converter, soft switching.

1. Introduction

The analysis of current research in the area of electronic converter applications leads to the conclusion that the trend is to move from drive applications to energy resource applications. It may be proved by the last publications of the distinguished Polish power electronic expert Prof. M.P. Kaźmierkowski [1–4]. The new converter configurations and new methods of control are useful to coupling different power sources (renewable) and nonlinear and asymmetric loads in one power line. One of the problem is realization of high efficiency DC-DC converters providing energy from a low voltage source (commercial fuel cells, most of photovoltaage panels) to high DC voltage suitable for an inverter. The required converter gain may exceed the value of 10 and the converter input current achieving substantial value involves significant power losses which prevent achieving high system efficiency. Among many solutions presented in the literature [5–8], when safety isolation is not required, the topology described in [9] and [10] whose scheme is presented in Fig. 1 seems to be interesting.

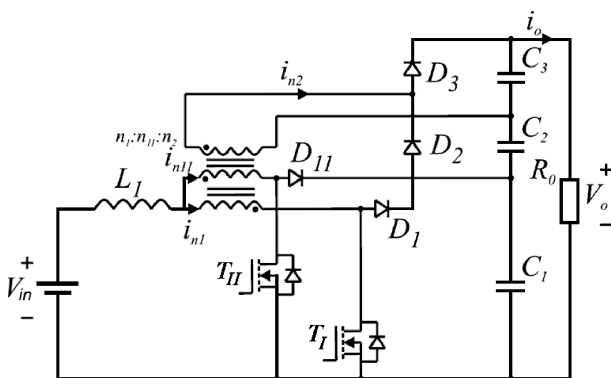


Fig. 1. Converter proposed in Ref. 9

Unfortunately, the converter switching frequency is limited to several dozens (50 kHz) because of the transistor hard switching process (switching power losses).

The transistor soft switching process may be realized by substituting the PWM (pulse width modulation) method of control by the PWM-FM (pulse width modulation by frequency regulation) method of control and introducing capacitors C_s parallel to the transistors. The switching frequency in this solution may achieve several hundred kHz. Such competitive proposition ensuring safety isolation is described in this article and presented in Fig. 2.

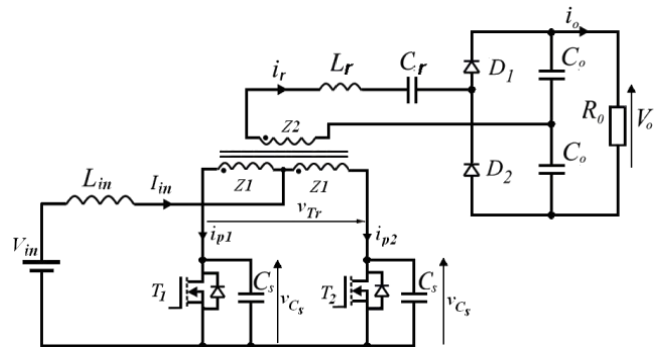


Fig. 2. Discussed push-pull resonant converter

The converter is a member of the class E resonant converters [12–14]. Similarly to the non-isolated model presented in Fig. 1, this converter may operate with duty cycle higher or lower than 50%.

2. Principle of operation

The principle of the converter operation is based on the charge process of the shunt capacitors C_s . After switching OFF the transistors, the capacitor is charged and next discharged before switching ON the transistor to provide transistor zero voltage switching process. The converter is controlled by changes of the transistor control pulses time, so both the frequency and duty ratio D are changed. With the control frequency suitable to the operation on the border between the buck and boost modes (Fig. 3a) the duty ratio $D = 50\%$. With the control

*e-mail: s.jalbrzykowski@pb.edu.pl

frequency lower than in Fig. 3a the duty ratio $D > 50\%$ and transistor control pulses overlap during the time when converter operates in the boost mode (Fig. 3b). With the control frequency higher than in Fig. 3a the duty ratio $D < 50\%$ and the dead time t_d occurs between transistors control pulses, a converter operates in the buck mode (Fig. 3c).

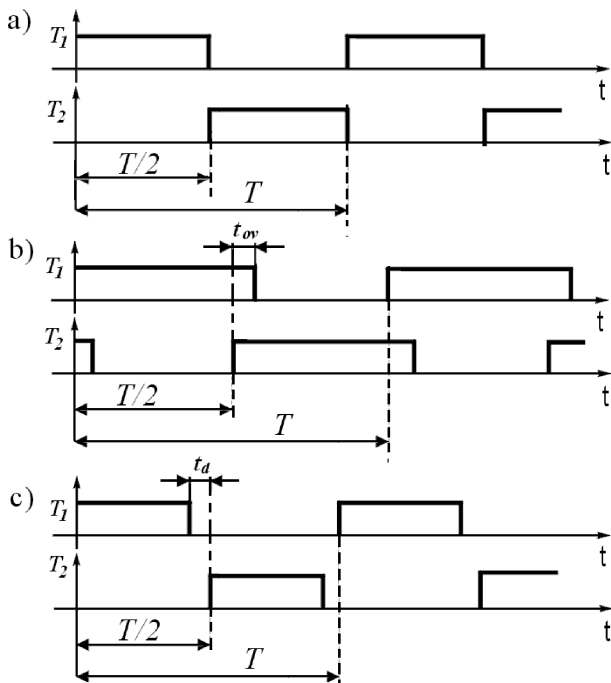


Fig. 3. The converter transistor control pulses for different operation modes: a) border between boost and buck, b) boost, c) buck

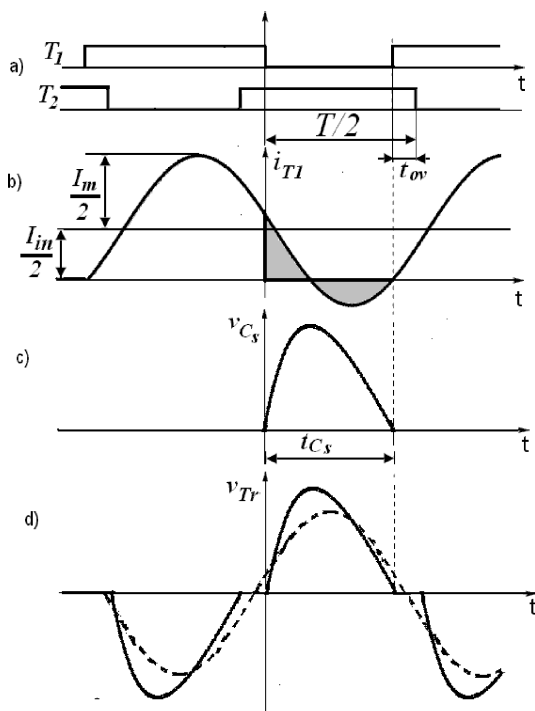


Fig. 4. The converter waveforms characteristic for the nominal point operation: a) transistor control 1 pulses, b) transistor and capacitor currents, c) transistor voltage, d) primary transformer voltage

The maximal power value is transferred by the converter with the minimal control frequency during the boost mode operation and for this point of operation the converter is designed. The characteristic current and voltage waveforms for this point of operation are presented in Fig. 4.

3. Mathematical description of the converter

Because the converter represents a strongly non-linear system, its description bases on the first harmonic components of the converter variables. Thus, it is assumed that the resonant circuit $L_r C_r$ current has sinusoidal waveform and the converter input current is constant.

The current of one of the primary transformer branches i_{p1} consists of a sinusoidal waveform (equal to half-value of the primary transformer current I_m) and a constant waveform (equal to half-value of the input current I_{in}). Part of this current, marked as the shaded part, flows through the capacitor C_s . Thus, the capacitor voltage can be described by the equation:

$$v_{C_s} = \frac{1}{C_s} \int_0^t \left(\frac{I_{in}}{2} - \frac{I_m}{2} \sin \omega x \right) dx \quad (1)$$

$$= \frac{P_{in}}{2\omega C_s V_{in}} \left[\omega t - \frac{1 - \cos \omega t}{\sin \varphi} \right],$$

where V_{in} – input source voltage, P_{in} – input Power, $\sin \varphi = \frac{I_{in}}{I_m}$.

According to Fig. 4 the transistor can be turned on after time t_{C_s} when the capacitor voltage takes zero value. For this point the following equation is fulfilled:

$$\sin \varphi = \frac{1 - \cos \omega t_{C_s}}{\omega t_{C_s}} \quad (2)$$

and because $t_{C_s} = \frac{T}{2} - t_{ov} = \frac{T}{2} (1 - w)$ where $w = \frac{t_{ov}}{T/2}$ – relative value of the overlap time.

$$\sin \varphi = \frac{1 + \cos w\pi}{\pi (1 - w)}. \quad (3)$$

The last equation expresses the dependence between mutual relation of the converter currents $\frac{I_{in}}{I_m}$ and the transistor control pulse overlap w .

In the steady state operation the capacitor voltage mean value during a half-period is equal to the input source voltage V_{in}

$$\frac{2}{T} \int_0^{t_C} v_{C_s} dt = V_{in}. \quad (4)$$

Based on Eq. (1), the capacitance C_s value as a function of the converter power and the coefficient of the control pulse overlap can be calculated

$$C_s = \frac{P_{in}}{4\pi^2 V_{in}^2} \left[\frac{\cos^2 w\pi - 1}{2 \sin^2 \varphi} + \frac{\sin w\pi}{\sin \varphi} \right]. \quad (5)$$

Table 1
Calculated converter parameters

Parameter	$\sin \varphi$	C_s	a_1	b_1	V_{Trm}	R_S	$Im(Z_r)$	L_r	C_r
Value	0.7	22 nF	167 V	68.8 V	180 V	18 Ω	22.4 Ω	31.6 μ H	36nF
No. equation	(3)	5)	(7a)	(7b)	(8)	(10)	(11)	k=1.5	

The capacitor voltage waveform determines the primary voltage of the transformer (see Fig. 4). The first harmonic component of the transformer voltage can be described in the form:

$$v_{Tr} = a_1 \cos \omega t + b_1 \sin \omega t, \quad (6)$$

where a_1, b_1 – decomposition coefficients:

$$a_1 = \frac{P_{in}}{2\pi^2 C_s V_{in} f} \cdot \left[\pi(1-w) \left(\sin w\pi + \frac{1}{2\sin \varphi} - \sin \varphi \right) + \frac{1}{\sin \varphi} \left(\frac{\sin 2w\pi}{4} - \sin w\pi \right) \right], \quad (7a)$$

$$b_1 = \frac{P_{in}}{2\pi^2 C_s V_{in} f} \cdot \left[\sin w\pi \left(1 + \frac{\sin w\pi}{2\sin \varphi} \right) - \cos w\pi \left(\frac{1}{\sin \varphi} - \pi(1-w) \right) - \frac{1}{\sin \varphi} \right], \quad (7b)$$

$$V_{Trm} = \sqrt{a_1^2 + b_1^2}. \quad (8)$$

The amplitude of the output transformer voltage is equal to $V_{Trm} \frac{z_2}{2z_1}$, where z_1, z_2 – the number of transformer turns.

The amplitude of the transformer output current is equal to $\frac{z_1}{z_2} I_m$.

The diode rectifier loaded by the resistance R_o can be expressed by the substitute resistance R_S with the same power.

$$\left(\frac{z_1}{z_2} \frac{I_m}{\sqrt{2}} \right)^2 R_S \eta_p = V_o I_o. \quad (9)$$

Taking into account the relation between the input $\frac{z_1}{z_2} I_m$ and output I_o rectifier current we can determine the substitute

resistance R_S

$$R_S = \frac{2}{\eta_p \pi^2} R_o. \quad (10)$$

The imaginary part of the resonance circuit impedance can be calculated, using the following equation.

$$Im(\widehat{Z}_r) = \omega L_r - \frac{1}{\omega C_r} = \sqrt{\left(\frac{\frac{z_2}{2z_1} V_{Trm}}{\frac{z_1}{z_2} I_m} \right)^2 - R_S^2}. \quad (11)$$

The resonant circuit pulsation $1/\sqrt{L_r C_r}$ should be smaller than the control pulsation, and if we assume proportion coefficient as $k = \omega \sqrt{L_r C_r}$, the resonant circuit characteristic impedance can be evaluated basing on Eq. (11).

$$\sqrt{\frac{L_r}{C_r}} = \frac{Im(\widehat{Z}_r)}{k - \frac{1}{k}}. \quad (12)$$

The above derived equations are useful for the calculation of the converter elements and parameters. The property value of the coefficient k should be evaluated in a converter simulation process.

The calculation example. The calculation concerns the following input dates. $V_{in} = 48$ V, $I_{in} = 20$ A ($P_{in} = 960$ W), $f = 215$ kHz, $w = 0.37$, $R_o = 90\Omega$, $Z_2/Z_1 = 3$. Calculation results, Table 1.

4. The P-spice simulation results

The calculated converter parameters were verified by simulation process using P-spice models of the transistors IRFP90N20D and diodes HFA25tb60. Adequate parameters are presented in the Table 2.

The characteristic waveforms for different points of converter operation are demonstrated in Fig. 5.

The voltage gain of the converter as a function of control frequency is plotted in Fig. 6.

Table 2
Simulated converter parameters

Parameter	$\sin \varphi$	C_s	V_{Trm}	R_S	$Im(Z_r)$	L_r	C_r
Value	0.68	14.7 nF+ C_{tp}^*	160 V	18 Ω	17.3 Ω	24.5 μ H	47 nF

C_{tp}^* – the transistor IRFP90N20D parasitic capacitance.

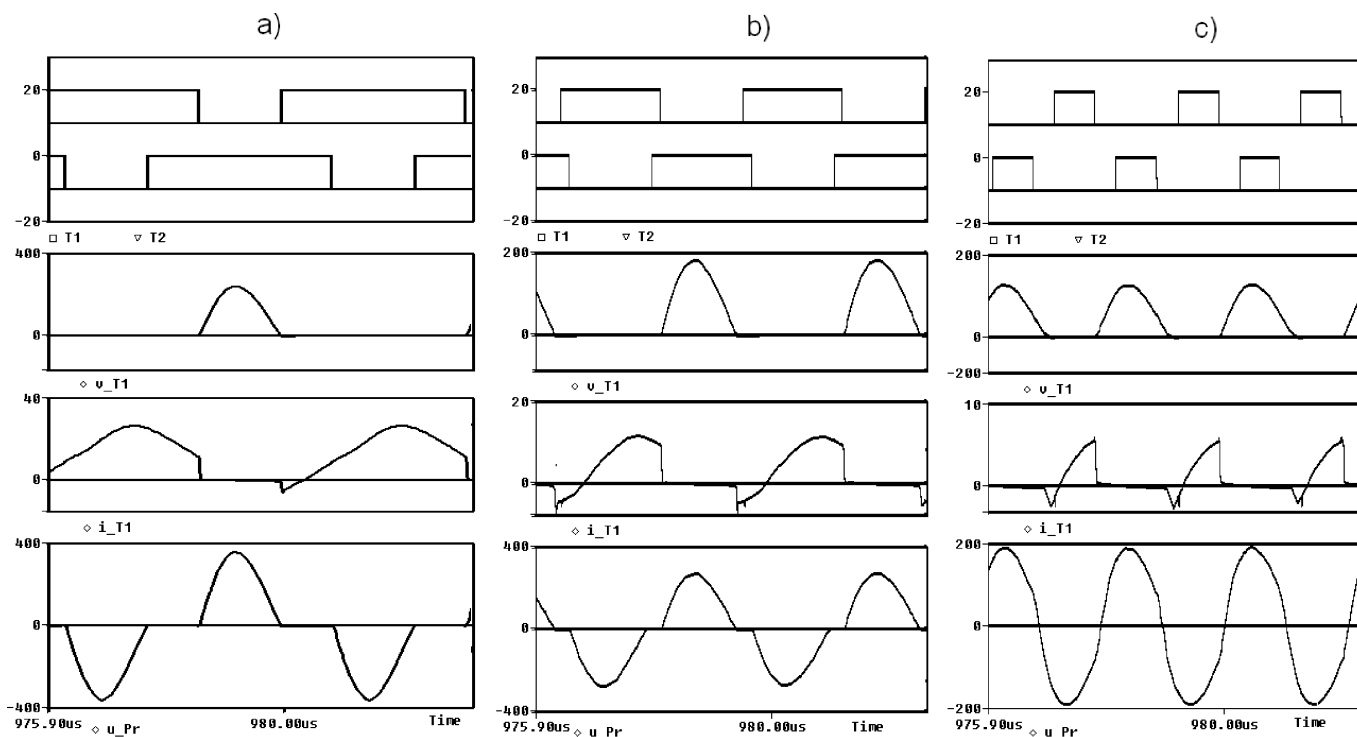


Fig. 5. Characteristic waveforms - simulation results: a) boost mode ($f = 215$ kHz), b) border between boost and buck modes ($f = 345$ kHz), c) buck mode (500 kHz). T_1, T_2 transistor control pulses, v_{T1} - transistor voltage, i_{T1} - transistor current, v_{Tr} - secondary transformer voltage

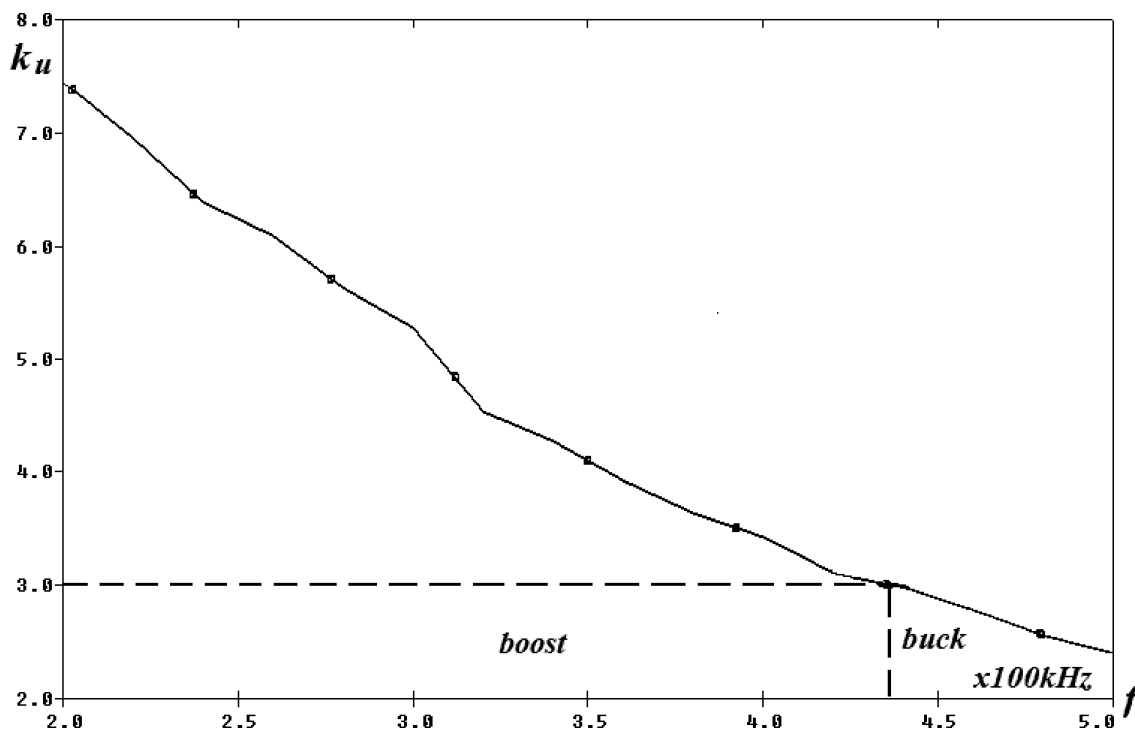


Fig. 6. The converter voltage gain as function of control frequency (simulation results)

Push-pull resonant DC-DC isolated converter

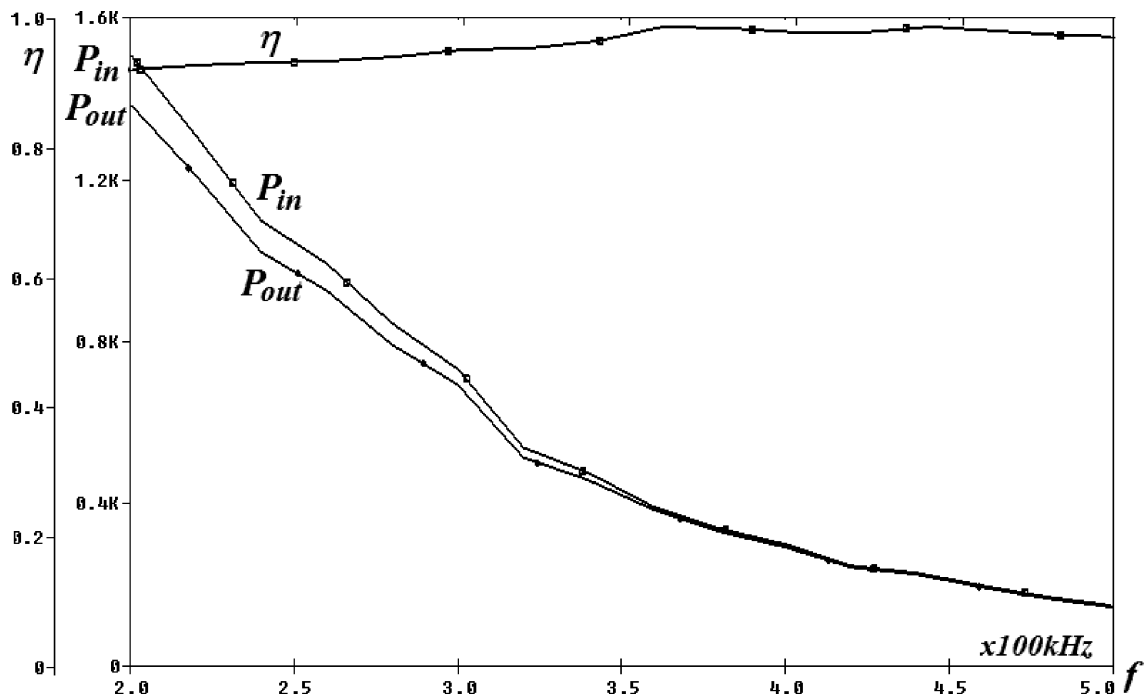


Fig. 7. The converter input and output power and its efficiency as function of control frequency- simulation results

Finally, the converter input and output power and efficiency as a function of control frequency is shown in Fig. 7.

5. Experimental results

The converter prototype was made using: transistors IRFP90N20D, diodes HFA25TB60, transformer implemented with 10X3 turns (Litz wires, 2 as primary and 3, in series, as secondary) on a Vitroperm 500F WAC T60004-L2130-W352 core, the resonant circuit was composed of an air coil (Litz wire) and polypropylene capacitors.

The essential differences between the measured and simulated results are involved with real (not ideal) elements, such as: transformer, inductors and capacitors used in practice. The measured waveforms characteristic for different modes are presented in Fig. 8.

The converter gain, as a function of the control frequency, is plotted in Fig. 9, and the converter output power and efficiency are plotted in Fig. 10.

The important characteristic property concerns the converter efficiency which remains constant with power changes.

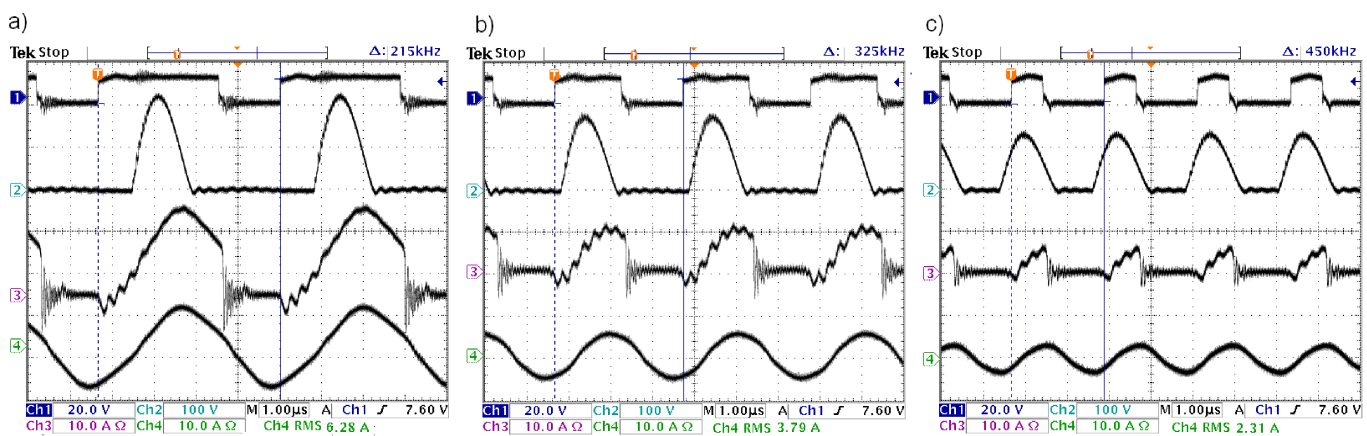


Fig. 8. Characteristic waveforms – experimental results: a) boost mode ($f = 215$ kHz), b) border between boost and buck modes ($f = 325$ kHz), c) buck mode (450 kHz). 1 – transistor control pulse (20 V/div), 2 – transistor voltage (100 V/div.), 3 – transistor current (10 A/div.) 4 – resonant circuit current (10 A/div.). Time (1 μ s/div.)

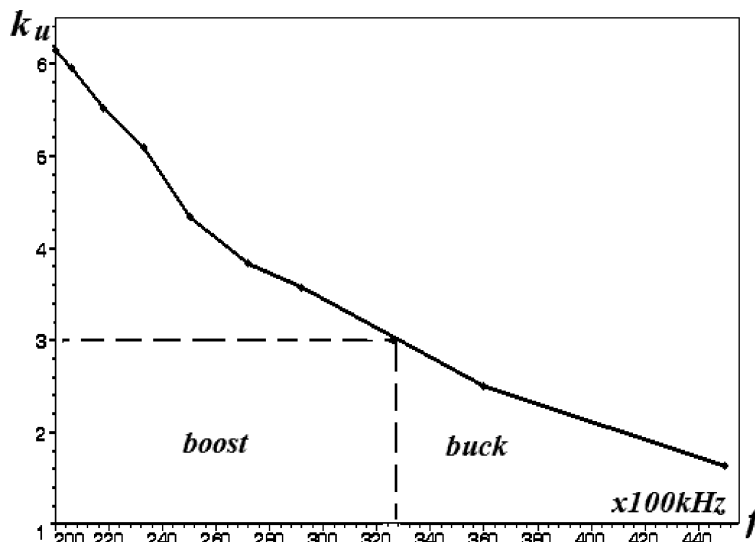


Fig. 9. The converter voltage gain as function of control frequency – experimental results

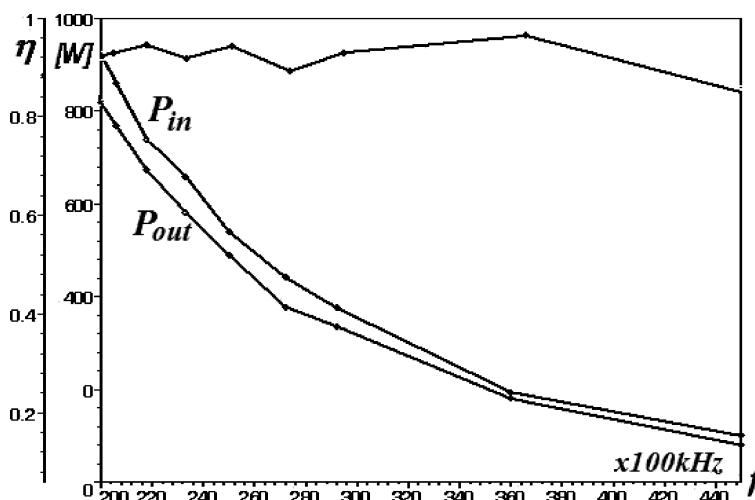


Fig. 10. The converter input and output powers and its efficiency as function of control frequency -experimental results

6. Conclusions

This paper describes the DC/DC converter with a high range of voltage gain regulation. It operates in the boost and buck modes of operation. The converter efficiency is comparably high thanks to the use of only two transistors on the high current side and the elimination of transistor switching losses by means of an adequate method of converter control (PWM FM). The simulation and experimental results confirm well enough the introduced mathematical model of converter operation based on the first harmonic of the voltage and current waveforms.

Acknowledgements. This paper is supported by the fund scientific project S/WE/3/2013.

REFERENCES

- [1] P. Antosiewicz and M.P. Kaźmierkowski, “Virtual – flux- based predictive direct power control of AC/DC converters with on-line inductance estimation”, *IEEE Trans. Ind. Electron.* 55, 4381–4389 (2008).
- [2] M. Malinowski, S. Styński, W. Kołomyjski, and M.P. Kaźmierkowski, “Control of three level PWM converter applied to variable – speed – turbines”, *IEEE Trans. Ind. Electron.* 56, 69–77 (2009).
- [3] J. Mordewicz and M.P. Kaźmierkowski, “Contactless energy system with FPGA – controlled resonant converter”, *IEEE Trans. Ind. Electron.* 57, 3181–3190 (2010).
- [4] M.P. Kaźmierkowski, M. Jasiński, and G. Wrona, “DSP-based-control of grid – connected power converters operating under grid distortions”, *IEEE. Ind. Informatics IEEE Trans.* 7, 204–211 (2011).
- [5] E.H. Kim and B.H. Kwon, “High step-up resonant push-pull converter with high efficiency” *Power Electronics IET 2*, 79–89 (2009).
- [6] M. Nymand and M.A.E. Andersen, “A new approach to high efficiency in isolated boost converters for high power low-voltage fuel cell applications”, *Power Electronic and Motion Control Conf. 13thEPE-PEMC 2008* 1, 127–131 (2008).

Push-pull resonant DC-DC isolated converter

- [7] R.J. Wai and R.Y. Duan, "High efficiency DC/DC converter with voltage gain electric power applications", *IEEE Proc.* 152, 793–802 (2005).
- [8] Q. Zhao and F.C. Lee, "High- efficiency, high step-up DC-DC converters", *IEEE Trans. on Power Electron.* 18, 65–73 (2003).
- [9] P. Klimczak and S. Munk-Nilsen, "Comparative study on paralleled vs. scaled DC-DC converters in high voltage gain applications", *Power electronic and Motion Control Conf. EPE-PEMC 2008 13th* 1, 108–113 (2008).
- [10] G.V. Torico-Bascope, R.P. Torico-Bascope, D.S. Oliviera, F.L.M. Antunes, S.V. Araujo, and C.G.C. Branco "A generalized high voltage gain boost converter based on three-state switching cell", *32nd Annual Conf. IEEE Industrial Electronics Society IECoN'06* 1, 1927–1932 (2006).
- [11] A. Tomaszuk and A. Krupa, "High efficiency high step-up DC-DC converters review", *Bull. Pol. Ac.: Tech.* 59 (4), 475–483 (2011).
- [12] S. Jalbrzykowski and T. Citko "Current-fed resonant full-bridge boost DC/AC/DC converter", *IEEE. Trans. on Ind. Electron.* 55 (3), 1198–1205 (2008).
- [13] S. Jalbrzykowski and T. Citko, "A bidirectional DC-DC converter for renewable energy systems", *Bull. Pol. Ac.: Tech.* 61 (2), 363–368. (2009).
- [14] M. Mikołajewski, "A self-oscillating H.F power generator with a Class E resonant amplifier", *Bull. Pol. Ac.: Tech.* 61 (2), 527–534 (2013).